Available online at www.sciencedirect.com
SCIENCE DIRECT
Journal of Molecular Catalysis A: Chemical 249 (2006) 71–79
JOURNAL OF MOLECULAR CATALYSIS A: CHEMICAL
www.elsevier.com/locate/molcata

Influence of the nature of the noble metal on the lean C_3H_6-assisted decomposition of NO on $Ce_{0.68}Zr_{0.32}O_2$-supported catalysts

Cyril Thomas [a,*], Olivier Gorce [a,1], Françoise Villain [b,c], Gérald Djéga-Mariadassou [a]

[a] *Laboratoire de Réactivité de Surface, UMR CNRS 7609, Université Pierre et Marie Curie, 4 Place Jussieu, Case 178, 75252 Paris Cedex 05, France*
[b] *Laboratoire de Chimie Inorganique et Matériaux Moléculaires, UMR CNRS 7071, Université Pierre et Marie Curie, 4 Place Jussieu, 75252 Paris Cedex 05, France*
[c] *Laboratoire pour l'Utilisation du Rayonnement Electromagnétique (LURE), Centre Universitaire Paris-Sud BP34, 91898 Orsay Cedex, France*

Received 15 November 2005; accepted 5 January 2006
Available online 8 February 2006

Abstract

The Selective Catalytic Reduction (SCR) of NO_x assisted by C_3H_6 is investigated on $Ce_{0.68}Zr_{0.32}O_2$ (CZ)-supported Platinum Group Metals (PGMs: Pd, Rh, Pt) catalysts.

This study shows that the order of reactivity of the PGMs supported on CZ is: Pd ≫ Pt ≥ Rh. The performances of the most active CZ-supported catalysts are comparable to those reported for SiO_2- or Al_2O_3-supported PGMs catalysts in terms of N_2 production. In contrast, the CZ-supported catalysts are much more selective to N_2 than those supported on SiO_2 or Al_2O_3, which makes them of particular interest. This difference of selectivity to N_2 of the CZ-supported catalysts suggests that the mechanism of the SCR of NO_x assisted by C_3H_6 proposed for Pd/CZ catalysts [C. Thomas, O. Gorce, C. Fontaine, J.-M. Krafft, F. Villain, G. Djéga-Mariadassou, Appl. Catal. B: Environ. 63 (2006) 201] is also valid for Pt or Rh/CZ catalysts. In this mechanism, ad-NO_2 species react with C_3H_6 to form ad-RNO_x compounds that further decompose to NO and oxygenates ($C_xH_yO_z$). The role of these oxygenates is to reduce the support to provide the sites responsible for NO decomposition to N_2 (Ce^{3+} surface cations).

The much higher activity of the Pd-based catalysts in the SCR of NO_x assisted by C_3H_6 might be attributed to the greater ability of the PdO_x phase to adsorb NO_2. This property might be assigned to the lower interaction of the PdO_x phase with CZ compared with that of the PtO_x or RhO_x phases.

Keywords: SCR of NO_x; Platinum Group Metals; C_3H_6; Ceria–zirconia; Catalysts

1. Introduction

Because of environmental concerns, the reduction of NO_x from lean exhausts sustains strong interest in the academic and industrial communities. Despite extensive investigations performed on this challenging issue, the catalyst able to comply with NO_x emission regulations on lean–burn internal combustion engines has still to be discovered [1]. A large number of catalysts have been evaluated in the Selective Catalytic Reduction (SCR) of NO_x by hydrocarbons [2,3]. Metal ion-exchanged zeolites, base metal oxides and supported Platinum Group Metals (PGMs) have received much interest in the SCR of NO_x [2]. However, the rather poor stability of metal ion-exchanged zeolites and the deactivation of base metal oxides in the presence of water in the feed constitute the main drawbacks of these catalysts to be used under real automotive exhausts [2]. On the other hand, supported PGMs exhibit rather low selectivity to N_2, N_2O being formed in substantial amounts [3]. Although not regulated, it must be emphasised that this pollutant is a well-known powerful greenhouse gas [4,5].

PGMs have mostly been supported on SiO_2 or Al_2O_3 [3] and very little attention has been paid to other supports such as ceria–zirconia. To our knowledge, only three studies have been reported for such catalysts for the SCR of NO_x by propene by: (i) Orlik et al. on $Rh/CeZrO_2$ [6], (ii) Centi et al. on $Pt/Ce_{0.50}Zr_{0.50}O_2/Al_2O_3$ [7] and (iii) Liotta et al. on $Pt/Ce_{0.50}Zr_{0.50}O_2$ [8]. Recently, we reported on the performances of $Pd/Ce_{0.68}Zr_{0.32}O_2$ (Pd/CZ) catalysts in the SCR of

* Corresponding author. Tel.: +33 1 44 27 36 30; fax: +33 1 44 27 60 33.
E-mail address: cthomas@ccr.jussieu.fr (C. Thomas).
[1] Present address: Renault sas, Centre Technique de Lardy, 1 allée Cornuel, 91510 Lardy, France.

1381-1169/$ – see front matter © 2006 Elsevier B.V. All rights reserved.
doi:10.1016/j.molcata.2006.01.001

NO_x assisted by C_3H_6 [9]. These catalysts exhibited much higher selectivity to N_2 than Pd^0/SiO_2. This difference was assigned to the occurrence of a deNO_x mechanism on Pd/CZ different from that of the dissociation of NO on zero-valent PGMs atoms [10].

This work reports on the influence of the nature of the PGMs (Pd, Rh, Pt) supported on CZ in the SCR of NO_x assisted by C_3H_6. The validity of the proposed mechanism for Pd/CZ catalysts [9] to other PGMs is discussed.

2. Experimental

2.1. Catalyst synthesis

2.1.1. Ceria–zirconia ($Ce_{0.68}Zr_{0.32}O_2$, CZ)

The CZ solid solution was provided by Rhodia. The CZ was added to a chloridric acid solution (pH 1.9) prepared by adding HCl to distilled water. After ageing for 2 h under vigorous stirring, CZ was filtered and washed with distilled water before being dried in air at 120 °C for 3 h. The samples were then reduced under pure H_2 (Air Liquide) for 2 h at 500 °C with a flow rate of 40 $mL_{NTP}\,min^{-1}$ of H_2 per gram of catalyst and finally gently exposed to air at RT. Such a preparation was performed for the sake of comparison with noble metal catalyst synthesis.

2.1.2. Rh/CZ

The CZ-supported rhodium catalyst (0.40 wt% Rh) was prepared by anionic exchange from an acidic solution of $RhCl_3{\cdot}3H_2O$ with the support [11]. The acidic solution of $RhCl_3{\cdot}3H_2O$ was added to an aqueous suspension of CZ (pH 1.9) prepared as described in Section 2.1.1. After being exchanged, Rh(0.40)/CZ was filtered and washed with distilled water before being dried in air at 120 °C for 3 h. This sample was then reduced under pure H_2 (Air Liquide) for 2 h at 500 °C with a flow rate of 40 $mL_{NTP}\,min^{-1}$ of H_2 per gram of catalyst and finally gently exposed to air at RT.

2.1.3. Pd/CZ

As already described [9], the two ceria–zirconia-supported Pd catalysts (0.54 and 0.89 wt% Pd) were prepared by incipient wetness impregnation of the chlorinated CZ by an aqueous solution of $PdCl_2{\cdot}3H_2O$ (Johnson Matthey). In these particular cases, the impregnations were carried out after exposure of the reduced CZ to air at RT (Section 2.1.1). After impregnation, the catalysts were aged for 2 h and dried in air at 120 °C for 3 h.

2.1.4. Rh-Pd/CZ

After exposure of a reduced Rh/CZ catalyst to air at RT, the Rh(0.44)Pd(0.54)/CZ catalyst was prepared by an impregnation procedure of Pd identical to that used for the preparation of the Pd/CZ catalysts (Section 2.1.3). After impregnation, the catalyst was aged for 2 h and dried in air at 120 °C for 3 h.

2.1.5. Rh-Pd/SiO_2

For comparison with Rh-Pd/CZ, a silica (Degussa, Aerosil 50)-supported Rh-Pd catalyst (0.40 wt% Rh and 0.44 wt% Pd) was prepared by subsequent incipient wetness impregnations of the support by aqueous solutions of $RhCl_3{\cdot}3H_2O$ and $PdCl_2{\cdot}3H_2O$ (Johnson Matthey). After impregnation, the catalyst was aged for 2 h and dried in air at 120 °C for 3 h.

2.1.6. Rh-Pt/CZ

The preparation of the Rh(0.44)Pt(0.91)/CZ was similar to that of Rh(0.44)Pd(0.54)/CZ (Section 2.1.4), except that an aqueous solution of $H_2PtCl_6{\cdot}6H_2O$ (Johnson Matthey) was used instead of that of $PdCl_2$ to carry out the impregnation of a Rh/CZ catalyst.

2.2. Catalyst characterisation

Metal and chlorine contents were determined by chemical analyses (CNRS—Vernaison). Chlorine contents were about 1 wt% for all CZ-supported catalysts.

The specific surface areas were determined by physisorption of N_2 at 77 K using a Quantasorb Jr. dynamic system equipped with a thermal conductivity detector (TCD). The specific surface areas were calculated using the BET method. The specific surface area of the CZ-supported catalysts was about 100 $m^2\,g^{-1}$ before and after testing, whereas that of Rh(0.40)Pd(0.54)/SiO_2 was about 50 $m^2\,g^{-1}$.

2.2.1. Determination of the percentage of exposed zero-valent metal atom (PEM^0)

With the well-known reducibility of the CZ support [12], the determination of the percentage of exposed zero-valent metal atom was done by means of hydrogenation reactions [13,14]. Benzene hydrogenation was used to titrate exposed zero-valent rhodium or platinum atoms, whereas propene hydrogenation was used to titrate exposed zero-valent palladium atoms [14].

Briefly, prior to benzene hydrogenation, the catalyst sample (50 mg deposited on sintered glass of a pyrex reactor) was heated in flowing H_2 (100 $mL_{NTP}\,min^{-1}$) at atmospheric pressure with a heating rate of 3 °C min^{-1} up to 500 °C and was kept at this temperature for 2 h. After cooling to 50 °C under H_2, the reaction was started. The partial pressure of benzene was 51.8 Torr, and the total flow rate was 107 $mL_{NTP}\,min^{-1}$ with H_2 as balance.

The procedure used for propene hydrogenation was similar to that of benzene hydrogenation except that the sample weight was 30–60 mg, the reduction temperature was 300 °C and the reaction temperature was −78 °C.

The composition of the effluents was analysed by means of on-line gas chromatographs (Hewlett-Packard 5890, FID) equipped with a paraffins-olefins-naphtenes-aromatics (PONA, HP, 50 m long, 0.20 mm inner diameter, 0.5 μm film thickness) or a CP-Al_2O_3/KCl (Chrompack, 50 m long, 0.32 mm inner diameter, 5 μm film thickness) capillary columns for benzene or propene hydrogenation, respectively. The only detected products were cyclohexane and propane.

From the initial reaction rates, the numbers of exposed zero-valent metal atoms were calculated according to turnover rates of 0.22 and 0.40 s^{-1} for benzene and propene hydrogenation reactions carried out at 50 and −78 °C, respectively [14].

2.2.2. XANES

X-ray absorption measurements were carried out using synchrotron radiation of the XAS13 station at LURE (Orsay, France) on-line D42 (May 3–4, 2001). Fluorescence yield spectra of Rh(0.44)Pd(0.54)/CZ were recorded at RT using a Ge solid detector (Eurisys, seven elements) combined with a multichannel analyser to select the Rh or Pd Kα fluorescences, whereas those of the reference compounds (Rh and Pd foils, 25 and 20 μm thick, respectively, Rh_2O_3 (>99.99% pure, Lancaster) and PdO (>99% pure, Lancaster)) were collected in the transmission mode. The incident beam was monochromatised using a Ge(4 0 0) double monochromator. XANES spectra were collected at the Rh and Pd K edges with a sampling step of 2.0 eV/point from 23,150 to 23,370 eV and from 24,300 to 24,500 eV, respectively, and an integration time of 10 and 2 s in fluorescence and transmission modes, respectively. The energy was calibrated using the Pd foil. XANES spectra were obtained from Rh(0.44)Pd(0.54)/CZ either after oxidation or reduction treatments under flowing air or H_2 (100 mL_{NTP} min^{-1}) for 2 h at 500 °C. To avoid the exposure of the reduced sample to O_2, the catalyst was then transferred into a UV cell (Suprasil quartz, 5 cm long, 1 cm wide and 1 cm high) that was finally sealed under vacuum (5×10^{-5} Torr). In a previous study [9], we checked that the high purity silica glass did not interfere with incident and fluorescent beams. The cell was set to 45° with respect to the incident RX beam and the fluorescence detector. The extraction of the data was done with Michalowicz's software package [15,16].

2.3. Catalytic runs

Prior to catalytic runs, the samples were calcined in situ in dry air at 500 °C (4 °C min^{-1}) for 2 h with a flow rate of 500 mL_{NTP} min^{-1} g^{-1} catalyst. Steady-state and temperature-programmed desorption (TPD) experiments were carried out. After being contacted with the appropriate gas mixture at RT, TPD experiments were carried out from RT to 500 °C with a heating rate of 10 °C min^{-1}. Before TPD experiments, the catalyst samples were flushed in N_2 to remove physisorbed species from the adsorption mixture.

These experiments were carried out in a U-type quartz reactor. The sample (0.2 g) was held between plugs of quartz wool and the temperature was controlled through a WEST 4000 temperature controller using a K type thermocouple. Reactant gases were fed from independent mass flow controllers (Brooks 5850E). The total flow was 250 mL_{NTP} min^{-1} to which corresponds a hour space velocity (HSV) of 112,500 h^{-1}.

Catalytic experiments were carried out with C_3H_6 as reductant. Typically, the composition of the C_3H_6–NO–O_2 reacting mixture was 1900 ppm C_3H_6, 340 ppm NO and 8% O_2 in N_2. These reactants were fed from independent gas cylinders (Air Liquide) of N_2 diluted gas mixtures.

The reactor outflow was continuously analysed using the combination of four different detectors. An Eco Physics CLD 700 AL chemiluminescence NO_x analyser (for NO and total NO_x (i.e. NO + NO_2)) allowed the simultaneous detection of both NO and NO_x. Two Ultramat 6 IR analysers were used to monitor N_2O, CO and CO_2. A FID detector (Fidamat 5A) was used to follow the concentration of hydrocarbons. We checked that under our experimental conditions, CO and CO_2 had a negligible response on the N_2O IR analyser, whereas that of C_3H_6 was significant. C_3H_6 contribution to the N_2O signal was taken into account to calculate the "true" N_2O concentration ($[N_2O]$) as follows (Eq. (1)):

$$[N_2O] = [N_2O]_{meas.} - \frac{[N_2O]^0 \times [C_3H_6]_{meas.}}{[C_3H_6]_{inlet}} \quad (1)$$

where $[N_2O]^0$, $[C_3H_6]_{inlet}$, $[C_3H_6]_{meas.}$ and $[N_2O]_{meas.}$ are the concentrations of N_2O due to the contribution of the inlet concentration of C_3H_6, the inlet concentration of C_3H_6, C_3H_6 and N_2O concentrations measured in the course of the reaction, respectively. As N_2 was used as balance, the conversion of NO_x to N_2 was calculated assuming 100% nitrogen mass balance (Eq. (2)):

$$\text{Conversion of } NO_x \text{ to } N_2\ (\%) = \frac{[NO_x]_{inlet} - ([NO_x]_{outlet} + 2[N_2O])}{[NO_x]_{inlet}} \quad (2)$$

where $[NO_x]_{inlet}$ and $[NO_x]_{outlet}$ are the concentrations of NO_x at the inlet and at the outlet of the reactor, respectively.

3. Results

3.1. Catalyst characterisation

3.1.1. Determination of the percentage of exposed zero-valent metal atoms (PEM^0)

Table 1 lists the percentage of exposed zero-valent metal atoms of CZ-supported Rh and Pd catalysts. As reported in previous studies from our group [11,17], CZ-supported Rh catalysts scarcely exhibit exposed zero-valent rhodium atoms. On the other hand, the existence of exposed zero-valent palladium atoms, under the present experimental conditions of propene

Table 1
Determination of the percentage of exposed zero-valent metal atoms (PEM^0) over $Ce_{0.68}Zr_{0.32}O_2$ (CZ) supported catalysts by means of benzene and propene hydrogenation reactions [14]

Catalysts	Rh(0.40)/CZ	Pd(0.54)/CZ[a]	Pd(0.89)/CZ[a]	Rh(0.44)Pd(0.54)/CZ	Rh(0.44)Pt (0.91)/CZ
Rh^0 (%)	2	–	–	0	0
Pd^0 (%)	–	17	16	18	–
Pt^0 (%)	–	–	–	–	3

[a] Data reported from Ref. [9] for comparison purpose.

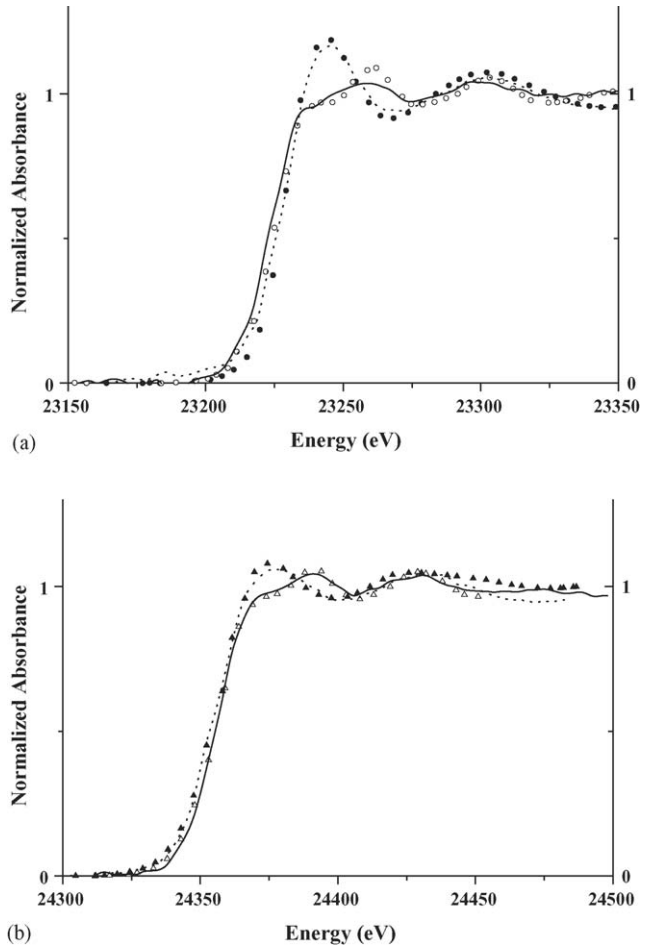

Fig. 1. XANES spectra (a) at the Rh K edge for Rh_2O_3 (●), the Rh foil (◯) and Rh(0.44)Pd(0.54)/CZ (calcined in air at 500 °C (- - -) or reduced in H_2 at 500 °C (—)); (b) at the Pd K edge for PdO (▲), the Pd foil (△) and Rh(0.40)Pd(0.54)/CZ (calcined in air at 500 °C (- - -) or reduced in H_2 at 500 °C (—)).

hydrogenation, is obvious. The percentage of exposed zero-valent palladium atoms is close to 17% for all catalysts. As already suggested [9], it is therefore very likely that after the calcination step, Pd was present as PdO.

The fairly low benzene hydrogenation activity of Rh(0.44)Pt(0.91)/CZ is assigned to Pt only (Table 1). The synthesis of this catalyst was carried out starting with the same Rh/CZ catalyst precursor as that used for the preparation of Rh(0.44)Pd(0.54)/CZ, the rhodium contribution of which to benzene hydrogenation is null (Table 1).

3.1.2. XANES measurements

XANES spectra of Rh(0.44)Pd(0.54)/CZ after calcination or reduction are shown in Fig. 1. The shape of the XANES spectrum at the Rh K edge after calcination of the sample closely resembles that of the Rh_2O_3 oxide reference (Fig. 1a). This suggests similar oxidation state and local geometry of Rh to those of Rh_2O_3. Surprisingly, the shape of the XANES spectrum of the bimetallic catalyst after reduction differs markedly from that of the Rh foil (Fig. 1a). Such a behaviour, which is also observed on Rh(0.40)/CZ [18], is attributed to the formation of electro-deficient Rh clusters owing to electronic perturbations induced on the metal by the reduced support, as also reported by Bernal et al. in the case of Pt/CeO_2 catalysts [19]. On the other hand, the comparison of the shape of the XANES spectra of the bimetallic sample at the Pd K edge either after calcination or after reduction correspond fairly well to those of the PdO and the Pd metal references (Fig. 1b), respectively. As for Pd(0.54)/CZ [9], this suggests that Pd is present as PdO clusters in the CZ-supported Pd catalyst. Interestingly, as identical comments stand for the bimetallic catalyst and the monometallic ones, it might be concluded that the metals do not seem to interact in the Rh(0.44)Pd(0.54)/CZ bimetallic catalyst.

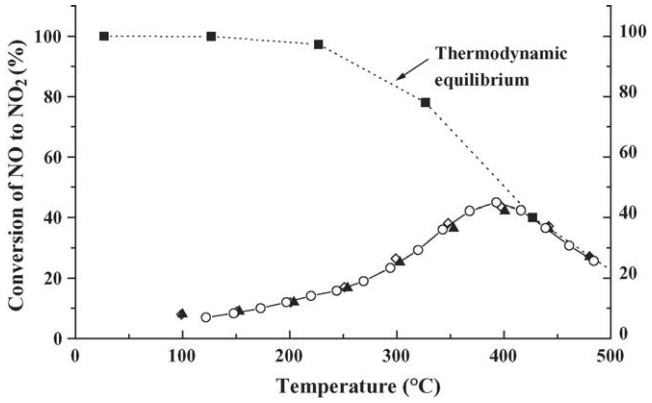

Fig. 2. Steady-state catalytic conversion of NO to NO_2 in the course of the NO–O_2 reaction (340 ppm–8%, balance N_2): (◊) $Ce_{0.68}Zr_{0.32}O_2$ (CZ), (◯) Rh(0.40)/CZ and (▲) Rh(0.44)Pd(0.54)/CZ.

3.1.3. NO oxidation

The NO oxidation reaction, which has been assumed of key importance in lean deNO_x catalysis [9,20–23], was investigated over different catalysts under steady-state conditions. Fig. 2 shows that NO oxidation is the greatest at 400 °C and decreases at higher temperatures because of thermodynamic limitations. It must be emphasised that the addition of PGMs does not enhance NO oxidation, as was also the case for Pd(0.89)/CZ [9], and this reaction is only catalysed by CZ.

3.1.4. Adsorption of NO–O_2–TPD in N_2 or in C_3H_6–O_2

The TPD profiles in N_2 or C_3H_6–O_2 obtained after exposure of CZ and Pd(0.89)/CZ to NO–O_2 (340 ppm–8% O_2 in N_2) have been described in details in previous articles [9,23]. The TPD traces found on Rh(0.40)/CZ and Rh(0.44)Pd(0.54)/CZ (not shown) are similar to those of CZ and Pd(0.89)/CZ [9], respectively. For all catalysts, NO_2 is the major NO_x desorbed species of the TPD in N_2, whereas NO is the chief product of the TPD in C_3H_6–O_2 (Table 2). The amounts of adsorbed NO_x species correspond well to those desorbed for the TPD in N_2, whereas the nitrogen balance of the TPD in C_3H_6–O_2 indicates that part of the stored NO_x transform to N_2 in the presence of C_3H_6 in the gas feed (Table 2). The interaction of pre-adsorbed NO_x with C_3H_6 was revealed on Rh(0.40)/CZ and Rh(0.44)Pd(0.54)/CZ (not shown), as was the case with CZ and Pd(0.89)/CZ [9]. However, this interaction occurred up to higher temperatures for Rh(0.44)Pd(0.54)/CZ than for Rh(0.40)/CZ (not shown), as

Table 2
Amounts of adsorbed or desorbed NO_x ($NO + NO_2$) and desorbed N_2O in the course of the TPD experiments after exposure of the catalysts to $NO–O_2$ (340 ppm–8%) in N_2

Catalysts	Experiment	Amounts of adsorbed (ads.) or desorbed (des.) species (10^{-5} mol g^{-1})						
		T_{NO_2} [a]	$NO_{x\,ads.}$ [b]	$NO_{des.}$	$NO_{2\,des.}$	$NO_{x\,des.}$	$N_2O_{des.}$	N balance[c]
CZ[d]	TPD in N_2	115	54.8	8.1	46.5	54.6	0.0	0.1
	TPD in $C_3H_6–O_2$		48.2	19.0	7.8	26.8	5.8	4.9
Rh(0.40)/Z	TPD in N_2	123	53.6	9.9	41.0	50.8	0.0	1.4
	TPD in $C_3H_6–O_2$		63.8	26.1	9.2	35.2	8.5	5.8
Pd(0.89)/CZ[d]	TPD in N_2	136	47.6	6.2	36.4	42.7	0.0	2.5
	TPD in $C_3H_6–O_2$		51.8	20.3	5.1	25.4	5.4	7.8
Rh(0.44)Pd(0.54)/CZ	TPD in N_2	135	45.5	7.5	37.4	44.9	0.0	0.3
	TPD in $C_3H_6–O_2$		57.8	23.9	8.2	32.1	6.4	6.5

[a] Temperature (°C) of the maximum of the first NO_2 desorption peak from the TPD in N_2 after adsorption of $NO–O_2$.
[b] The moderate fluctuation of the amount of adsorbed NO_x is related to slightly different times of exposure and not to differences in the starting conditions.
[c] N balance calculated with respect to N_2 equivalent.
[d] Data reported from Ref. [9] for comparison purpose.

was found for Pd(0.89)/CZ compared with CZ [9]. Similar to Pd(0.89)/CZ, the first NO_2 desorption peak of the TPD in N_2 of Rh(0.44)Pd(0.54)/CZ is shifted to higher temperatures compared with those of CZ and Rh(0.40)/CZ (Table 2).

3.1.5. Steady-state $C_3H_6–NO–O_2$ reaction

Fig. 3 shows the performances of the catalysts for the SCR of NO_x under steady-state conditions with stepwise increase of the temperature. The temperature of maximum of N_2 formation and the corresponding NO_x and C_3H_6 conversions are listed in Table 3. The main effect of the introduction of PGMs is to enhance C_3H_6 activation as the T_{50} C_3H_6 (temperature at 50% conversion of C_3H_6) of the CZ-supported PGMs catalysts decrease significantly compared with CZ (Table 3). It must also be emphasised that C_3H_6 oxidation is steeper on Rh(0.40)Pd(0.54)/SiO_2 than on the CZ-supported catalysts (Fig. 3).

Except Rh(0.40)/CZ, which shows low deNO_x activity comparable to that reported by Orlik et al. on a similar catalyst [6], CZ-supported PGMs catalysts exhibit much higher deNO_x activity than CZ. The selectivity to N_2 is, however, very comparable for all CZ-based materials and remains higher than 80% at maximum NO_x to N_2 conversion (Table 3). Conversely, the selectivity to N_2 of Rh(0.40)Pd(0.54)/SiO_2 is much lower and is of about 50%. Supported Pd catalysts are the most efficient in lean deNO_x, whereas Rh(0.40)/CZ is the less active of the CZ-supported PGMs catalysts.

It is worthwhile to report that the sum of the SCR of NO_x to N_2 of Rh(0.40)/CZ and Pd(0.54)/CZ corresponds well to that of Rh(0.44)Pd(0.54)/CZ (Fig. 4a). Regarding the bimetallic catalysts, the deNO_x activity of Rh(0.44)Pd(0.54)/CZ (Fig. 3e) is higher than that of Rh(0.44)Pt(0.91)/CZ (Fig. 3f), which clearly shows that Pt is less active than Pd in the SCR of NO_x when supported on CZ. The picture is less obvious for the comparison of Rh and Pt as the deNO_x activity of a monometallic Pt catalyst was not investigated in the present work. Nevertheless, the comparison of the deNO_x activity of Rh(0.40)/CZ and the difference of that of Rh(0.44)Pt(0.91)/CZ with that of Rh(0.40)/CZ may be informative on that particular point. Fig. 4b shows that the activity of Pt, deduced from the above-mentioned difference, is close to that of Rh but takes place at lower temperature. For CZ-supported PGMs catalysts, the catalytic activities for the SCR of NO_x follow the order: $Pd \gg Pt \geq Rh$.

Finally, the introduction of 1.7 wt% water in the gas feed (not shown) at maximum deNO_x activity results in a moderate (10%) and reversible deactivation [9].

Table 3
Temperature of maximum of N_2 formation, percentage of NO_x converted to N_2 at this temperature, selectivity to N_2 at T_{max} N_2, C_3H_6 conversion at T_{max} N_2 and temperature at 50% conversion of C_3H_6 (T_{50} C_3H_6) over $Ce_{0.68}Zr_{0.32}O_2$ (CZ)- and SiO_2-supported catalysts for the steady-state $NO–O_2–C_3H_6$ reaction (340 ppm–8%–1900 ppm, N_2 balance)

Catalysts	T_{max} N_2 (°C)	NO_x to N_2 at T_{max} N_2 (%)	Selectivity to N_2 at T_{max} N_2 (%)[a]	C_3H_6 conversion at T_{max} N_2 (%)	T_{50} C_3H_6 (°C)
CZ	361	8	81	34	380
Rh(0.40)/CZ	318	9	83	30	355
Pd(0.54)/CZ	263	21	83	38	303
Pd(0.89)/CZ	243	29	87	50	243
Rh(0.44)Pd(0.54)/CZ	288	28	81	68	263
Rh(0.44)Pt(0.91)/CZ	289	16	85	45	294
Rh(0.40)Pd(0.44)/SiO_2	309	20	50	77	290

[a] Selectivity to N_2 referred to as $(N_2/(N_2 + N_2O) \times 100)$.

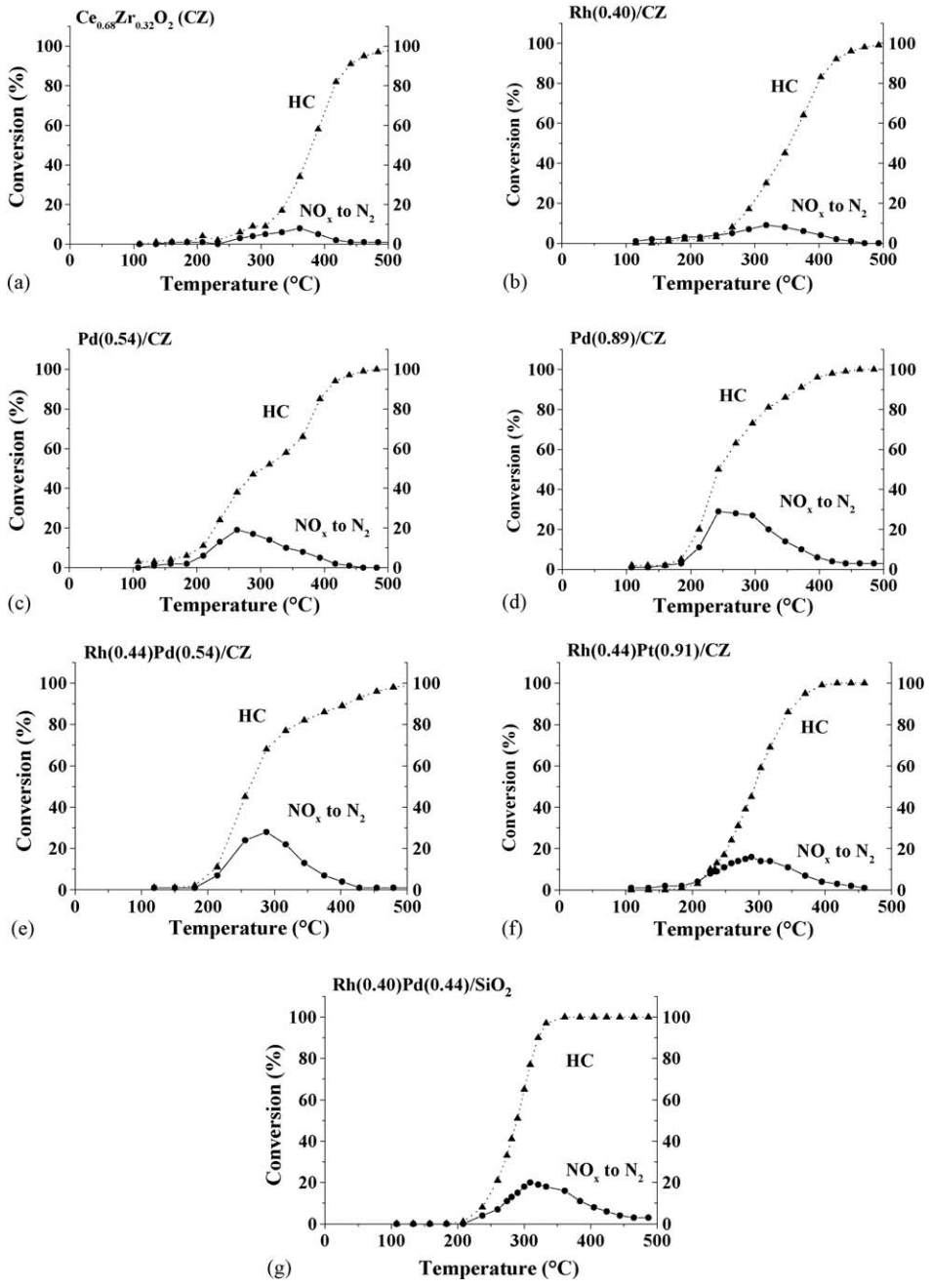

Fig. 3. Steady-state catalytic conversions of C_3H_6 and NO_x in the course of the C_3H_6–NO–O_2 reaction (1900 ppm–340 ppm–8%, balance N_2): (a) $Ce_{0.68}Zr_{0.32}O_2$ (CZ), (b) Rh(0.40)/CZ, (c) Pd(0.54)/CZ, (d) Pd(0.89)/CZ, (e) Rh(0.44)Pd(0.54)/CZ, (f) Rh(0.44)Pt(0.91)/CZ and (g) Rh(0.40)Pd(0.44)/SiO_2.

4. Discussion

The characterisation of the metallic phases, and hence of metal oxide phases, supported on ceria-based catalysts is a very challenging problem [24]. The characterisation of metal particles by means of H_2 or CO chemisorptions was not performed because it is well known that CZ-supported catalysts adsorb large amounts of these probe molecules and that the analysis of CO chemisorption faces stoichiometric problems [24]. In addition, the low contents of metal involved in the synthesised catalysts along with the elevated surface area of the CZ support prevented the use of TEM to obtain further information on the metallic phases deposited on CZ. To overcome these difficulties, the use of model hydrogenation reactions was considered to characterise the metallic phases, and hence the metal oxide phases indirectly. From these experiments (Table 1), it is obvious that the percentage of metal exposed as zero-valent metal atoms is much greater for Pd catalysts than for Rh or Pt ones. These results agree well with the work of Summers and Ausen in which these authors concluded to the greater interaction of Pt compared to that of Pd with CeO_2 [25]. Accordingly, the comparison of the XANES spectra of Pd and Rh catalysts (Refs. [9,18] and Fig. 1) shows that the reduction of Pd is easier than that of Rh for CZ-supported catalysts. These XANES spectra

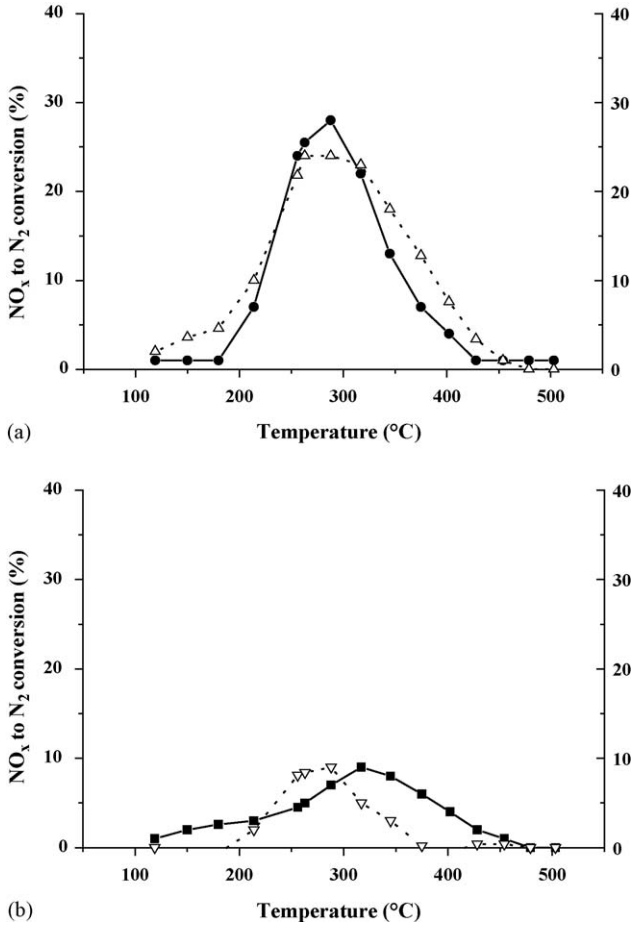

Fig. 4. NO_x to N_2 conversion of (a) Rh(0.44)Pd(0.54)/CZ (●) and the sum of those of Rh(0.40)/CZ and Pd(0.54)/CZ (△), and (b) Rh(0.40)/CZ (■) and the difference of those of Rh(0.44)Pt(0.91)/CZ and Rh(0.40)/CZ (▽) in the course of the C_3H_6–NO–O_2 reaction (1900 ppm–340 ppm–8%, balance N_2).

also reveal that Rh and Pd do not seem to interact with each other for the bimetallic catalyst (Section 3.1.2).

Qualitatively, the hydrogenation results suggest that the Pd metal particles, hence the size of the Pd metal oxide particles as only minor sintering effects are expected for reduction temperatures equal or lower than 500 °C [24], must be comparable or bigger than the Rh or Pt metal particles. It is, indeed, difficult to consider that the greater interaction of Pt or Rh compared to Pd with CeO_2 would lead to bigger metal particles in the case of the Pt or Rh catalysts, the latter catalysts yielding to the lower percentages of metal exposed as zero-valent metal atoms after reduction (Table 1).

The introduction of PGMs to CZ clearly promotes the activation of C_3H_6 and the deNO_x activity (Table 3). In addition, the selectivity to N_2 is much higher on the CZ-based materials compared with that found on SiO_2-supported zero-valent PGMs catalysts (Table 3 and Ref. [9]). The different N_2 selectivity obtained for CZ- and SiO_2-supported catalysts supports the assumption that the PGMs are stabilised as PGMs oxide phases (NMO_x) by CZ and do not undergo to complete reduction under the reacting mixture in agreement with the work of Liotta et al. on a Pt(1.0)/$Ce_{0.60}Zr_{0.40}O_2$ catalyst [8]. As recently reported [9], this discrepancy also suggests that the lean deNO_x mechanism occurring on the CZ-supported catalysts is different from that elucidated on supported zero-valent PGMs atoms by Burch et al. [10]. For Pd/CZ catalysts, a mechanism has been proposed [9]. Given that the selectivity to N_2 of the CZ-supported Rh and Pt catalysts closely resembles that of Pd/CZ and differs markedly from that of the corresponding supported zero-valent atoms [22,26–28], such a mechanism might be generalised to the CZ-supported PGMs catalysts studied in the present work (Fig. 5). In this mechanism, the SCR of NO_x proceeds through the interaction of NO_2 (cycle 1), adsorbed on the NMO_x catalytic function, with C_3H_6 to form RNO_x species that further decompose to oxygenates ($C_xH_yO_z$) and NO (cycle 2). These oxygenates act as reductants of CZ to create the catalytic sites responsible for the decomposition of NO to N_2 (cycle 3). This mechanism is supported by the adsorption–desorption experiments (Section 3.1.4) which show that: (i) NO is the major desorbed NO_x species of the TPD in C_3H_6–O_2, whereas NO_2 is the major desorbed species of the TPD in N_2. Such a result closely corresponds to gas phase experiments for which NO_2 is stoichiometrically transformed to NO in the presence of C_3H_6 along with the simultaneous formation of oxygenates [23]. (ii) The interaction of C_3H_6 with pre-adsorbed NO_2 species is most pronounced for CZ-supported Pd catalysts (Section 3.1.4) that exhibit the greatest deNO_x activities (Table 3).

NO decomposition on Ce^{3+} sites, resulting from the reduction of CZ (cycle 3) by the formed oxygenates, has originally been demonstrated by Niwa et al. [29] and confirmed later by other authors [30–32]. It is worthwhile reporting that this decomposition pathway has also been considered in three-way catalysis in which CO is used as reductant [33].

The occurrence of a deNO_x mechanism on CZ-supported PGMs catalysts different from that depicted on reduced PGMs atoms [10] is also supported by the order of reactivity observed for the CZ-supported PGMs materials: Pd ≫ Pt ≥ Rh. This reactivity order is indeed different from that found on SiO_2- or Al_2O_3-supported catalysts [34,35] among which supported Pt catalysts exhibit the greatest deNO_x activity and supported Rh ones the lowest activity. The deNO_x reactivity order reported for SiO_2-supported PGMs catalysts [34] is in good agreement with the specific activities found for C_3H_6 oxidation by Cant and Hall [36]. This similarity corroborates the fact that on zero-valent PGMs atoms, the SCR of NO_x proceeds through the dissociation of NO and the recombination of adsorbed N atoms to form N_2, the oxygen left from the NO dissociation process being cleaned by C_3H_6 oxidation [10]. In contrast, the reactivity order observed on CZ-supported PGMs catalysts suggests that PdO_x catalyses mild oxidation of C_3H_6 more readily than PtO_x or RhO_x do. Adsorption–desorption experiments (Section 3.1.4) indicate that this peculiarity might be attributed to the ability of the CZ-supported PdO_x phase to adsorb NO_2 compared with those of PtO_x or RhO_x and, thus, to form RNO_x species that further decompose to oxygenates being considered as the real reductants [37,38] of the SCR process (Fig. 5). This NO_2 adsorption discrepancy between the NMO_x phases might be correlated with the lower interaction of the PdO_x phase with CZ compared with those of RhO_x and PtO_x. The indirect evidence

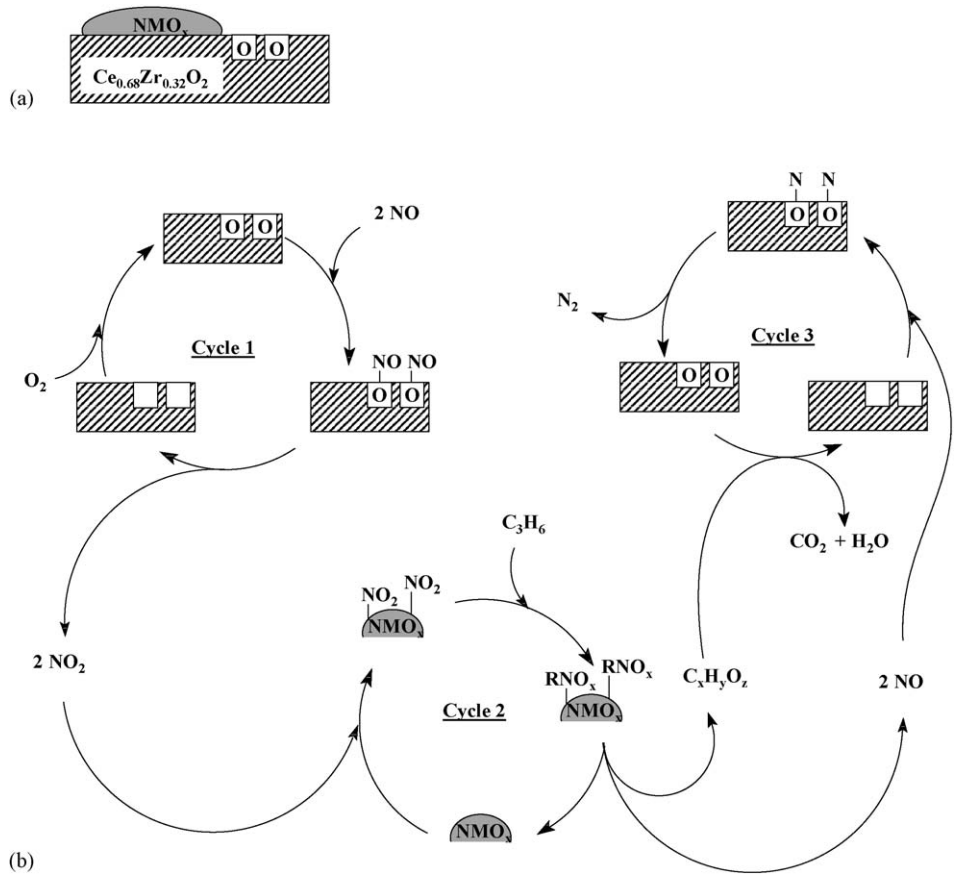

Fig. 5. (a) Schematic representation of the catalytic functions, NMO_x representing PGMs oxide phases and (b) mechanism of the lean C_3H_6-assisted decomposition of NO over PGMs/$Ce_{0.68}Zr_{0.32}O_2$ (CZ) catalysts, $\boxed{O}$, RNO_x, $C_xH_yO_z$ representing an oxygen from the surface of the CZ support, organic nitrogen-containing and oxygenates compounds of undefined composition, respectively [9].

of which is provided by the XANES measurements (Fig. 1 and Refs. [9,18]) showing that the PdO_x phase is more easily reduced than the RhO_x one. The higher interaction of Pt compared to that of Pd with CeO_2 has been revealed by Summers and Ausen through CO-FTIR investigations [25]. By means of CO-FTIR and HRTEM measurements, Bernal et al. also concluded to strong interaction between Pt and CeO_2 [19].

At first sight, the SCR of NO_x activities found for the Pd-based catalysts of this study do not favourably compare with those reported on SiO_2- or Al_2O_3-supported PGMs catalysts. Nevertheless, it must be pointed out that the SCR of NO_x activities of the present study correspond to the selective transformation of NO_x to N_2, whereas literature data mainly report on global activities including the production of both N_2 and N_2O [28,34,39–43]. For some of the aforementioned studies, N_2 selectivity has not been reported [28,39–42]. As it is well established that the selectivity to N_2 hardly exceeds 50% in the temperature range of interest on supported zero-valent PGMs catalysts [22,26–28], the SCR of NO_x to N_2 activities found in the present study (Table 3) are very comparable to those of supported zero-valent PGMs catalysts. Therefore, this makes the Pd/CZ catalytic systems of greater interest than the SiO_2- or Al_2O_3-supported PGMs ones because of their much lower production of N_2O, the formation of which is to be avoided from a global warming point of view [4,5]. The SCR of NO_x to N_2 activities obtained in the present work are slightly lower than those reported by Centi et al. [7] or Liotta et al. [8] for CZ-based Pt catalysts. In contrast, these catalysts were slightly less selective to N_2 than ours. These studies were, however, realised with lower C_3H_6 and O_2 concentrations, with lower HSV and with higher NO concentration than ours. These differences in reaction conditions make the comparison difficult as we noticed that increases of C_3H_6 and NO concentrations and decreases of the O_2 concentration and the HSV resulted in an increase of the SCR activity (not shown).

5. Conclusion

This study shows that the order of reactivity of the PGMs supported on CZ is: $Pd \gg Pt \geq Rh$. The performances of the most active CZ-supported catalysts are comparable to those reported for SiO_2- or Al_2O_3-supported PGMs catalysts in terms of N_2 production. In contrast, the CZ-supported catalysts are much more selective to N_2 than those supported on SiO_2 or Al_2O_3, which makes them of particular interest. This difference of selectivity to N_2 of the CZ-supported catalysts suggests that the mechanism of the SCR of NO_x assisted by C_3H_6 proposed for Pd/CZ catalysts [9] is also valid for Pt or Rh/CZ catalysts.

In this mechanism, ad-NO_2 species react with C_3H_6 to form ad-RNO_x compounds that further decompose to NO and oxygenates ($C_xH_yO_z$). The role of these oxygenates is to reduce the support to provide the sites responsible for NO decomposition to N_2 (Ce^{3+} surface cations).

The much higher activity of the Pd-based catalysts in the SCR of NO_x assisted by C_3H_6 might be attributed to the greater ability of the PdO_x phase to adsorb NO_2. This property might be assigned to the lower interaction of the PdO_x phase with CZ compared with that of the PtO_x or RhO_x phases.

Although appreciable SCR of NO_x to N_2 is achieved on the CZ-supported catalysts, enhancement of the activities is still needed to comply with most recent emission regulations. The proposed deNO_x mechanism (Fig. 5), whose obvious complexity lies in the fact that the three catalytic cycles have to turn over simultaneously, suggests ways in which deNO_x activity could be improved. Superior activity in the NO oxidation reaction is to be obtained (Fig. 5, cycle 1), as the evaluated catalysts do not allow for maximum production of NO_2 that remains far from thermodynamic equilibrium at maximum N_2 formation (Fig. 2). Improvement of the selective mild oxidation of C_3H_6 remains a very challenging task (Fig. 5, cycle 2), as this moderate oxidation process always competes with total oxidation [44]. The quality of the catalytic sites responsible for the decomposition of NO (Fig. 5, cycle 3) might also be considered. These different issues are currently being investigated in our group.

Acknowledgments

Rhodia contributed to part of the financial support for this work; the Ministère de l'Enseignement Supérieur et de la Recherche organisation supported the work of Dr. O. Gorce (Grant 98-4-10713). We also thank G. Blanchard for his interest in this work and P. Lavaud for his invaluable help in technical support.

References

[1] R.J. Farrauto, R.M. Heck, Catal. Today 55 (2000) 179.
[2] V.I. Pârvulescu, P. Grange, B. Delmon, Catal. Today 46 (1998) 233.
[3] R. Burch, J.P. Breen, F.C. Meunier, Appl. Catal. B: Environ. 39 (2002) 283.
[4] Y. Traa, B. Burger, J. Weitkamp, J. Chem. Soc. Chem. Commun. 21 (1999) 2187.
[5] J. Perez-Ramirez, F. Kapteijn, K. Schoffel, J.A. Moulijn, Appl. Catal. B: Environ. 44 (2003) 117.
[6] S.N. Orlik, V.L. Struzhko, T.V. Mironyuk, G.M. Tel'biz, Theor. Exp. Chem. 37 (2001) 311.
[7] G. Centi, P. Fornasiero, M. Graziani, J. Kašpar, F. Vazzana, Topics Catal. 16–17 (2001) 157.
[8] L.F. Liotta, A. Longo, A. Macaluso, A. Martorana, G. Pantaleo, A.M. Venezia, G. Deganello, Appl. Catal. B: Environ. 48 (2004) 133.
[9] C. Thomas, O. Gorce, C. Fontaine, J.-M. Krafft, F. Villain, G. Djéga-Mariadassou, Appl. Catal. B: Environ. 63 (2006) 201.
[10] R. Burch, P.J. Millington, A.P. Walker, Appl. Catal. B: Environ. 4 (1994) 65.
[11] F. Fajardie, J.-F. Tempère, J.-M. Manoli, O. Touret, G. Blanchard, G. Djéga-Mariadassou, J. Catal. 179 (1998) 469.
[12] S.H. Overbury, D.R. Mullins, in: A. Trovarelli (Ed.), Ceria Surfaces and Films for Model Catalytic Studies Using Surface Analysis Techniques, Imperial College Press, London, 2002, p. 328.
[13] F. Fajardie, J.-F. Tempère, G. Djéga-Mariadassou, G. Blanchard, J. Catal. 163 (1996) 77.
[14] L. Salin, C. Potvin, J.-F. Tempère, M. Boudart, G. Djéga-Mariadassou, J.-M. Bart, Ind. Eng. Chem. Res. 37 (1998) 4531.
[15] A. Michalowicz, Logiciels pour la chimie, Société Française de Chimie, Paris, 1991, p. 102.
[16] A. Michalowicz, J. Phys. IV France 7 (1997) 235.
[17] I. Manuel, J. Chaubet, C. Thomas, H. Colas, N. Matthess, G. Djéga-Mariadassou, J. Catal. 224 (2004) 269.
[18] C. Fontaine, C. Thomas, J.-M. Krafft, O. Gorce, F. Villain, G. Djéga-Mariadassou, in preparation.
[19] S. Bernal, G. Blanco, J.M. Gatica, C. Larese, H. Vidal, J. Catal. 200 (2001) 411.
[20] C. Yokoyama, M. Misono, J. Catal. 150 (1994) 9.
[21] T. Okuhara, Y. Hasada, M. Misono, Catal. Today 35 (1997) 83.
[22] K.O. Haj, S. Ziyade, M. Ziyad, F. Garin, Appl. Catal. B: Environ. 37 (2002) 49.
[23] O. Gorce, F. Baudin, C. Thomas, P. Da Costa, G. Djéga-Mariadassou, Appl. Catal. B: Environ. 54 (2004) 69.
[24] S. Bernal, J.J. Calvino, J.M. Gatica, C. López Cartes, J.M. Pintado, in: A. Trovarelli (Ed.), Chemical and Nanostructural Aspects of the Preparation and Characterisation of Ceria and Ceria-Based Mixed Oxide-Supported Metal Catalysts, Imperial College Press, London, 2002, p. 85.
[25] J.C. Summers, S.A. Ausen, J. Catal. 58 (1979) 131.
[26] T. Tanaka, T. Okuhara, M. Misono, Appl. Catal. B: Environ. 4 (1994) L1.
[27] R. Burch, T.C. Watling, Catal Lett. 37 (1996) 51.
[28] R. Burch, T.C. Watling, Appl. Catal. B: Environ. 11 (1997) 207.
[29] M. Niwa, Y. Furukawa, Y. Murakami, J. Colloid Interface Sci. 86 (1982) 260.
[30] A. Martinez-Arias, J. Soria, J.C. Conesa, X.L. Soane, A. Arcoya, R. Cataluna, J. Chem. Soc. Faraday Trans. 91 (1995) 1679.
[31] S.H. Overbury, D.R. Mullins, D.R. Huntley, Lj. Kundakovic, J. Catal. 186 (1999) 296.
[32] M. Daturi, N. Bion, J. Saussey, J.-C. Lavalley, C. Hedouin, T. Seguelon, G. Blanchard, Phys. Chem. Chem. Phys. 3 (2001) 252.
[33] G. Djéga-Mariadassou, F. Fajardie, J.-F. Tempère, J.-M. Manoli, O. Touret, G. Blanchard, J. Mol. Catal. A: Chem. 161 (2000) 179.
[34] R. Burch, P.J. Millington, Catal. Today 29 (1996) 37.
[35] G.R. Bamwenda, A. Ogata, A. Obuchi, J. Oi, K. Mizuno, J. Skrzypek, Appl. Catal. B: Environ. 6 (1995) 311.
[36] N.W. Cant, W.K. Hall, J. Catal. 16 (1970) 220.
[37] G. Djéga-Mariadassou, Catal. Today 90 (2004) 27.
[38] G. Djéga-Mariadassou, M. Boudart, J. Catal. 216 (2003) 89.
[39] J. Li, J. Hao, L. Fu, T. Zhu, Topics Catal. 30–31 (2004) 81.
[40] H. Shinjoh, T. Tanabe, K. Yokota, M. Sugiura, Topics Catal. 30–31 (2004) 319.
[41] R. Burch, T.C. Watling, Catal Lett. 43 (1997) 19.
[42] T. Okuhara, Y. Hasada, M. Misono, Catal. Today 35 (1997) 83.
[43] R. Burch, J.A. Sullivan, T.C. Watling, Catal. Today 42 (1998) 13.
[44] J. Haber, W. Turek, J. Catal. 190 (2000) 320.